ADVANCED FUNCTIONAL MATERIALS
www.afm-journal.de

Pattern Formation of Silver Nanoparticles in 1-, 2-, and 3D Microstructures Fabricated by a Photo- and Thermal Reduction Method

By *Jong-Jin Park,* Xavier Bulliard, Ji Min Lee, Jaehyun Hur, Kyuhyun Im, Jong-Min Kim, Prem Prabhakaran, Namchul Cho, Kwang-Sup Lee,* Sung-Yong Min, Tae-Woo Lee, Son Yong,* and *Dong-Yol Yang*

One-, two-, and three-dimensional microstructures with dispersed silver nanoparticles are fabricated by a combination of photopatterning and thermal treatment from a silver salt containing photosensitive epoxy resin. Ultraviolet photo-irradiation and subsequent thermal treatment are combined to control the rate of silver salt reduction, the size and the arrangement of nanoparticles, as well as the reticulation of the epoxy resin. This approach allows the creation of high resolution 1-, 2-, and 3D patterns containing silver nanoparticles, with a homogeneous distribution of nanoparticles regardless of the irradiated area.

1. Introduction

The arrangement of nanoparticles in 1-, 2-, or 3D is critical to harness their unique electrical, optical and magnetic properties. Phenomena such as light propagation in nanoparticles crystals[1] and plasmonic resonance[2] are highly dependent on the specific position of nanoparticles. For the optimization of device performance, crucial parameters include the nanoparticle size and the interparticle distance, as well as the arrangement controlling the coupling effects. Recent developments in self-assembly techniques have opened interesting perspectives to create motifs with desirable interparticle distance.[3] Methods such as reverse micelles, microemulsions, Langmuir-Blodgett films, organometallic techniques, and two-phase liquid–liquid systems[4–8] have been used for 2D nanoparticle patterning on a substrate. Other techniques, such as micro-contact printing,[9] direct deposition by photochemical decomposition[10,11] and inkjet printing,[12] offer a valuable complement for fabrication. Among all architectures, the 3D arrangement of nanoparticles remains one of the most challenging goals due to stabilization problems. In order to create a mechanically robust 3D structure, nanoparticles must first be arranged through successive self-assembly and then sintered at elevated temperature. Another approach for the formation of stable 3D arrangements of nanoparticles with proper interparticle distance is to embed them in a matrix, typically a polymer. This approach has limitations due to the complicated dispersion of nanoparticles in a viscous polymers or the aggregation of nanoparticles. In this study, we report complex 2D or 3D structures consisting of a fine dispersion of metal nanoparticles in a polymer matrix, using a combination of photo- and heat treatments of photosensitive nanoparticle precursors and a photosensitive polymer to build the desired structure.

The unique approach involved is the uniform growth of nanoparticles during the formation of the polymer pattern, occurring simultaneously to fabricate complex 2D and 3D architectures. Through UV or laser irradiation, metal nuclei were generated to form nanoparticles in the polymer matrix with the desired shape by selective crosslinking. Additional heat treatment in the second stage was used to control the final distribution of nanoparticles and crosslink polymer network completely. The approach allowed us to overcome the difficulties previously reported, such as aggregation or inhomogeneous dispersion of nanoparticles in a matrix, and to create complex structures with a good resolution, which could be used to fabricate micro- or nano-machines. Silver was chosen as the metal nanoparticle candidate in this study for its chemical and thermal stability, electrical conductivity and catalytic properties. Furthermore, it exhibits a surface plasmon absorption peak in the visible range of the color spectrum. Silver metal was formed from a salt precursor by photoreduction, thermal reduction or a combination of the two processes, as described in detail below. The nanoparticles were

[*] Dr. J.-J. Park, Dr. X. Bulliard, Dr. J. M. Lee, Dr. J. Hur, Dr. K. Im, Dr. J.-M. Kim
Samsung Advanced Institute of Technology, Mt.14-1, Nongseo-Dong, Giheung-Gu, Yongin-Si, Gyeonggi-Do 446-712 (Korea)
E-mail: jongjin00.park@samsung.com
Prof. K.-S. Lee, P. Prabhakaran, N. Cho
Department of Advanced Materials, Hannam University
Daejeon 306-791 (Korea)
E-mail: kslee@hnu.kr
Prof. T.-W. Lee, S.-Y. Min
Department of Materials Science and Engineering, Pohang University of Science and Technology
San 31 HyojaDong, Nam-gu, Pohang, Gyeongbuk 790-784 (Korea)
Prof. D.-Y. Yang, S. Yong
Department of Mechanical Engineering, KAIST
Daejon 305-701 (Korea)

DOI: 10.1002/adfm.201000055

synthesized in situ in an epoxy-based matrix (SU-8), preventing aggregation of the particles and, thus, allowing the fabrication of 2D or 3D objects.

2. Results and Discussion

The first step for the synthesis of nanoparticles was photoreduction, using pulse radiolysis through UV irradiation. In this method, a pulse of high energy electrons is applied to generate hydrated electrons and radicals in the metal salt solution. The reduced metal ions agglomerate, forming oligomeric clusters and finally colloidal metal particles.[13] The early steps of the reduction of the silver ion by hydrated electrons and H atoms in solution have been previously studied in solution and can be summarized as follows:[14,15]

$$Ag^+ + e^-_{aq} \rightarrow Ag^0 \text{ (atom formation)} \quad (1)$$

$$Ag^+ + H \rightarrow Ag^0 \text{ (atom formation)} \quad (2)$$

$$Ag^0 + Ag^+ \rightarrow Ag_2^+ \quad (3)$$

$$Ag_2^+ + Ag^+ \rightarrow Ag_3^{2+} \text{ (cluster formation)} \quad (4)$$

As metal particles form, they simultaneously act as a catalyst for the reduction of the remaining metal ions in the solution. When the cluster size reached about 10^2 to 10^3 atoms, a transition in the chemical and physical behavior of the clusters from molecular to bulk properties was observed.[16] As silver nanoparticles exhibit a characteristic extinction bands in the visible region of the extinction spectra, the change in color can be used as an indication of particle formation and growth. Ershov et al.[13,17] found that $Ag_2{}^+$ (265 and 310 nm), Ag_4^{2+} (265 nm), $Ag_1{}^0$ (360 nm), Ag_2^0 (270 nm), Ag_4^0 (340 nm) clusters were formed by photoreduction of silver.

In our experiments, the formation of nanoparticles was carried out in γ-butyrolactone (GBL) from silver trifluoroacetate (STA), in the absence of epoxy resin. Upon UV exposure, the solution changed from colorless to bright yellow and, finally, to yellow. The change of color was induced by surface plasmon resonance (SPR) resulting from the formation of metal colloids. The absorbance was measured as a function of UV exposure time, shown in Figure 1a. The absorption peak at 325 nm[18] peak increases sharply due to the homogeneous nucleation of silver nanoparticles in the solution, and its intensity increased further due to successive growth processes, including further reduction of Ag^+ ions and the subsequent aggregation between newly formed and previously existing Ag^0 particles. Although there is a slight red shift of the peak before and after UV exposure, a further peak shift occurred between 120 and 240 s of UV exposure. This suggests that once Ag^0 particles are formed, no significant increase of particle size occurs during the further UV irradiation. The TEM image in Figure 1b shows that nanoparticles formed with this technique had a narrow size distribution with an average diameter of 2.5 ± 1.0 nm. The increase in the SPR peak intensity observed is presumably due to the change of the concentration of Ag particles and not the increase in the particle size.

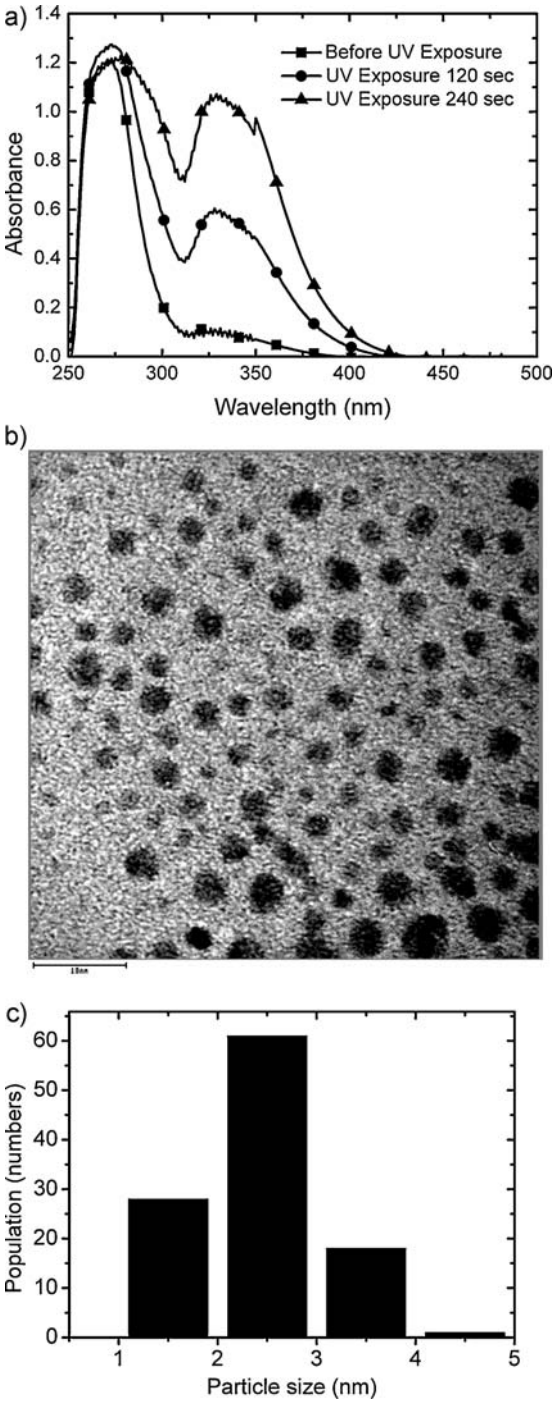

Figure 1. a) UV absorbance spectra after photo-induced reduction: 0 s (black), 120 s (red), and 240 s (blue) of UV exposure, b) TEM image of the reduced silver nanoparticles after 120 s of UV exposure (scale bar = 10 nm), and, c) distribution of silver nanoparticles formed after 120 s UV exposure; the average particle size and density were estimated to be 2.5 ± 1.0 nm and 0.067 nm^{-2}, respectively.

The second option for nanoparticle synthesis is thermal reduction. Among several possible compounds for metallic silver layer deposition, the best candidates are Ag(I) fluorinated or non-fluorinated carboxylates[19–21] that decompose below 673 K,

yielding metallic silver. In our case 3 wt% fluorinated carboxylate CF_3COOH in GBL was used. The decomposition of silver trifluoroacetate was observed at temperatures over 120 °C, resulting in the formation of Ag^0 and CF_3COOH, through a process similar to the thermal deposition of CH_3COOAg. The reduction process was promoted by longer heat treatment, as shown in Figure 2a, which represents the UV absorbance as a function of heat treatment time. At the same temperature, particles tended to grow up to a diameter of 5 nm, which may be attributed to melting fusion (agglomeration of smaller particles) processes owing to the relatively longer thermal treatment. As compared with photoreduction, thermal reduction led to a smaller number of nanoparticles nucleates ($0.067\,nm^{-2}$ for photoreduction and $0.050\,nm^{-2}$ for thermal reduction), but to nanoparticles with a larger final diameter because of agglomeration (2.5 ± 1.0 nm for photoreduction and 3.1 ± 1.2 nm for thermal reduction).

Another interesting approach is the combination of photo- and thermal reduction for silver nanoparticle synthesis. In the first stage, nanoparticle nucleation and growth was initiated by photoreduction upon UV exposure for 4 min, since many nanoparticles nucleates are formed with this process. In the second stage, a thermal treatment at 120 °C was applied for 2 min to promote the further growth of particles by diffusion. A solution composed of 8 wt% of STA in SU-8 resin was used for the experiments and results are shown in Figure 3. It should be noted that, since no thermal curing agent was added to the resin formulation, the two-stage process is necessary to fully crosslink the epoxy resin. The color of the solution was initially reddish, due to the presence of phenyl bonds on the epoxy resin. It then turned rapidly to yellow as nanoparticles formed and epoxy was cured. The main advantage of this process is that during UV exposure nanoparticles nucleated homogeneously in the resin. Simultaneous crosslinking of the resin impeded the rapid coalescence of freshly formed metal colloids, thus stabilizing the system. The polymer terminates the growth of the particles by controlling silver nucleation. In the second stage, during heat treatment, nanoparticles can further grow through a melting process and finally the matrix is fully crosslinked. Heat treatment thus did not impede the further grow of nanoparticles through the diffusion of ions or small nanoparticles, but coalescence of bigger nanoparticles was impeded by the crosslinked epoxy network, as shown in Figure 6a. Because of the conversion of monomer to polymer with nanoparticles, the viscosity of the medium increases and this leads to a decrease in the rates of the photo-polymerization and of melt diffusion in the matrix; thus an increase is observed in the concentration of small and separated nanoparticles. The characteristic plasmon absorption peak around 420 nm was observed in the UV-vis spectrum in Figure 3a. This is in good agreement with the results of previous investigations by Quinten.[22] The absorption band was broadened mainly due to the growth of particles by heat diffusion.[23] The size dependence of the SPR peak position is explained by a size-dependent dielectric constant of a metal particle due to the interactions of conduction electrons. Figure 3b shows TEM photographs and size distributions of the silver nanoparticles formed in the SU-8 matrix. The final size (4.5 ± 2.0 nm) of the silver nanoparticles was considerably larger, as compared with the case of photoreduction in Figure 1 and thermal reduction in Figure 2. For the same total process time, the combination of photo- and thermal reduction thus led to larger nanoparticles with a slightly broader size distribution. This is due to the effective nucleation of growth by the UV treatment and the coalescence of smaller nanoparticles toward larger ones during the heat treatment.

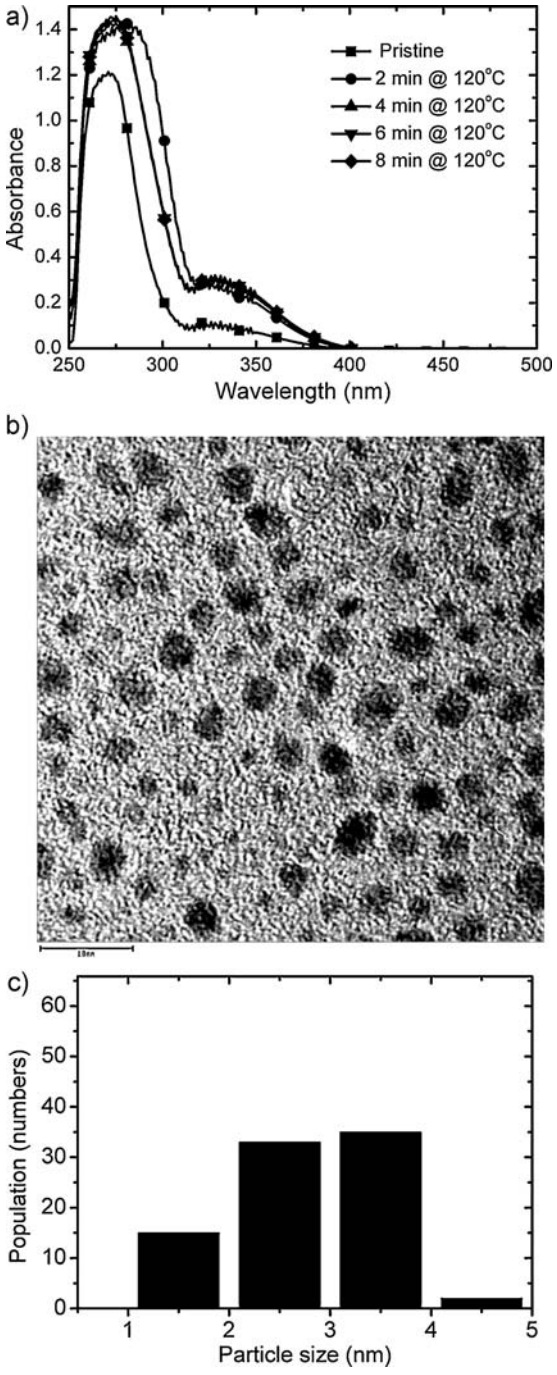

Figure 2. a) UV absorbance spectra after thermal induced reduction: 0 min (black), 2 min (red), and 4 min (blue), 6 min (green) and 8 min (pink) at 120 °C, b) TEM image of the reduced silver nanoparticles after thermal treatment of 2 min at 120 °C (scale bar = 10 nm), and, c) distribution of silver nanoparticles formed after 2 min of thermal treatment; the average particle size and density were estimated to be 3.1 ± 1.2 nm and $0.050\,nm^{-2}$, respectively.

Finally, the effect of nanoparticles on the crosslinking of epoxy matrix was analyzed. When nanoparticles are mixed with

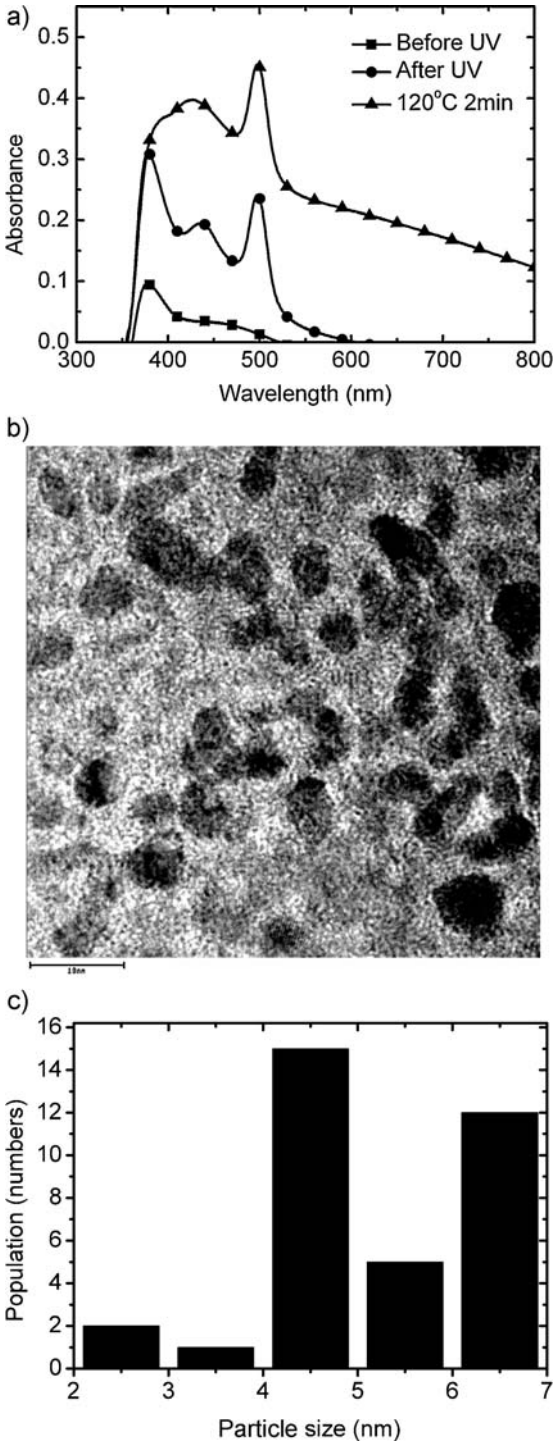

Figure 3. a) UV absorbance spectra after photo-induced reduction: before UV (black), and after 2 min of UV (red), and 2 min of thermal treatment at 120 °C (blue), b) TEM image of the reduced silver nanoparticles after both photo- and thermal treatments for 2 min (scale bar = 10 nm), and, c) distribution of silver nanoparticles formed after 2 min of thermal treatment; the average particle size and density were estimated to be 4.5 ± 2.0 nm and 0.029 nm^{-2}, respectively.

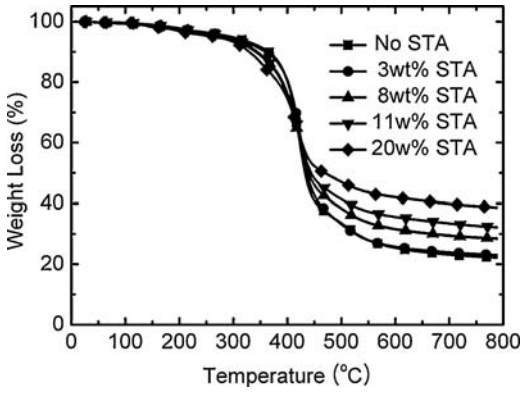

Figure 4. TGA for various silver contents in polymer matrix: 0 (blue), 3 (black), 8 (red), 11 (light blue), and 20 (light green) wt% of STA.

photo-curable resin, their high absorption alters the crosslinking process. In our study, the incident light absorption by nanoparticles was reduced because of the use of silver precursors. However the formation of nanoparticles still influenced the cationic polymerization of SU-8 by UV exposure. Figure 4 shows the thermal stability of polymer having various silver trifluoroacetate from 3 to 20 wt% in SU-8 epoxy, after UV exposure for 4 min followed by thermal curing at 120 °C for 2 min. The degree of polymerization of the epoxy resin in the presence of silver precursor appears to be lower compared to that of pristine monomer at 400 °C. At 3 wt% STA, the photocrosslinked pattern became a network, which was not dissolved in the developing solvent. Further thermal annealing at 120 °C is essential to fully cure the resin. The crosslinking points are formed around the silver nanoparticles, which are homogeneously formed initially into the polymer, and they may be confined in the polymer network knitted by crosslinking networks.

For the 2D microfabrication, the combination of UV curing for homogeneous nucleation and growth of nanoparticles in partially cured epoxy resin, and thermal curing to complete the crosslinking was used. With this procedure, we obtained uniform stripes with a width of 1.2 μm and a 5 μm pattern containing silver nanoparticles, as shown in Figure 5. This architecture was formed by spin-coating a blend containing 0.2 wt% STA and SU-8 resin in a solvent on a silicon wafer. The formed film was exposed to UV irradiation through a mask to cure the exposed regions, and baked to crosslink the UV-exposed area. The unexposed area is not affected by thermal curing and can be easily washed with GBL during the developing process to reveal the uniform patterns. In the stripes, nanoparticles were homogeneously dispersed, due to their stabilization by the epoxy network, as shown in Figure 5b. The remarkable advantage of this approach is the high resolution that can be attained by using nanoparticles precursors. This high resolution would not be possible by using pre-existing nanoparticles, as the absorption and scattering of incident light would lead to a partial dissolution of the lines during the developing process and a loss of lateral resolution. In this work, as silver nanoparticles are generated during UV exposure, there is little difficulty in fabricating high resolution structures because the light scattering is not prominent, as is the case for recipes involving nanoparticle dispersions. In the case of mixing nanoparticles with polymers, the light cannot even provide enough energy to crosslink the film

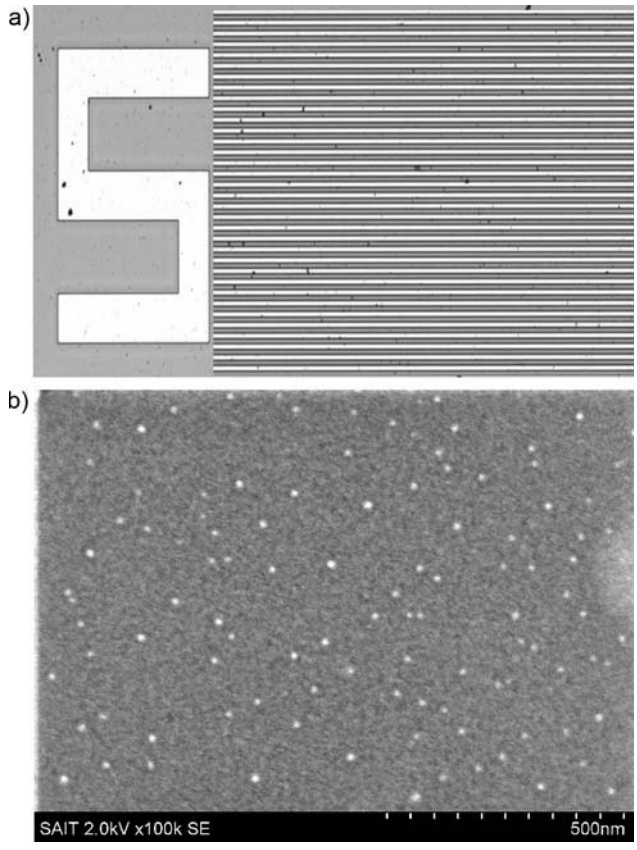

Figure 5. a) Optical microscopic image of pattern (silver particles are embedded in the brown regions) – the number "5" (left) and multiple lines (right) demonstrate the possibility of fabricating 2D and 1D silver particle-embedded patterns, respectively. b) SEM image of embedded silver nanoparticles in the pattern; the image was taken from the arbitrary brown region.

due to the absorbance of nanoparticles, for any exposure time. The cured polymer matrix easily terminates the growth of the nanoparticles in solid film when compared with such a change taking place in a solution phase, as shown in Figure 5. SU-8 epoxy polymer presents a significant steric barrier to the addition of silver nanoparticles to the surface of growing particles and thereby slows the growth kinetics. This is evident from the significant variation of the average sizes and shapes of the silver nanoparticles in the presence of polymers and silver-polymer interactions, as shown in Figure 3c.

After 2D fabrication, a procedure for 3D architectures fabrication containing well-dispersed nanoparticles was established. The components were similar to those used for 2D microfabrication, but UV reduction was replaced by laser-reduction for the solidification of the 3D matrix and the nucleation of nanoparticles. The photolysis process with nanosecond laser excitation has recently been confirmed for the synthesis of nanoparticles from a silver colloidal solution.[24–26] In our case, the process was tested on the epoxy and silver precursors system. In the first stage, experiments were carried out in 2D by using the cationic polymerization process. Results showing epoxy line patterns can be found in the Supporting Information. The formation of nanoparticles was confirmed, even though the resolution of patterns was partially lost in 2D because of intensive photo-reduction of metal ions in a volume as large as the focal volume (approximately 0.1 μm^3); the absorption of light is intensely confined within the focal volume, hence the photo-reduction of metal ions in this volume of 0.1 μm^3 resulted in locally higher silver nanoparticles. This led to a high concentration of nanoparticles and, in turn, to insufficient curing of the epoxy matrix. The procedure was in contrast perfectly adapted to the fabrication of 3D architectures containing homogeneously dispersed silver nanoparticles, as shown in Figure 6a. The formed micro-objects consisted of a 8×8 periodic structure of 6 μm height $\times$ 10 μm length $\times$ 10 μm width. It was formed by two-photon stereo-lithography, using highly efficient chromophores absorbing as photosensitizer, and baking post-exposure for 10 min at 90 °C. A high resolution SEM image of the wall of the 3D structure, shown in Figure 6a, highlights the formation and homogeneous dispersion of nanoparticles embedded in the cured epoxy resin. Note that the existence of silver atoms was confirmed by energy-dispersive X-ray spectroscopy (EDX) (Fig. 6b). This novel procedure combining soluble STA in a photo-polymerizable epoxy resin is a powerful approach for the fabrication of micro-objects with well-defined nanoscale features. After full curing, the objects are very stable and do not collapse up to high temperatures (150 °C). A silver nanoparticles-embedded SU-8 epoxy matrix can be achieved even at low silver concentrations (0.2 wt%). In in situ cationic polymerization, the formation of silver nanoparticle increases proportional to laser exposure time, up to 80 mW (see the Supporting Information Figure S1). The high molecular weight leads to a satisfactory extent of crosslinking, so the balance of exposure time (100 mW) and post-exposure baking (90 °C for 10 min) time are the key factor for successful fabrication in this experiment.

3. Conclusions

A series of 2D or 3D polymer structures containing well-dispersed nanoparticles were formed through in situ nucleation and growth of the particles in the matrix. A combination of photo-treatment and heat treatment was used for the simultaneous formation of nanoparticles and solidification of the polymer matrix. Since these two processes are competitive, the balance between photo-excitation and post-baking treatment is a critical parameter for the success of the procedure. In particular, the size of the nanoparticles, their concentration and distribution in the matrix can potentially be controlled. Since the thermal cross-linking of polymer matrix and growth of nanoparticles are competitive and simultaneous processes, there is an inherent limitation on the density of nanoparticles obtainable for a particular combination of particles and matrix. However, an important breakthrough here is that the in situ formation of nanoparticles has no effect on the formation of 2D or 3D architectures in terms of resolution. This emerging technique for nanocomposite materials formation may have a significant impact on electronic, optical, and electromechanical technologies, which could then be applied to periodic nanostructures for photonic crystals,[27] photonic meta materials replacing silver chemical vapor deposition[28] and substitution for SU-8 MEMS

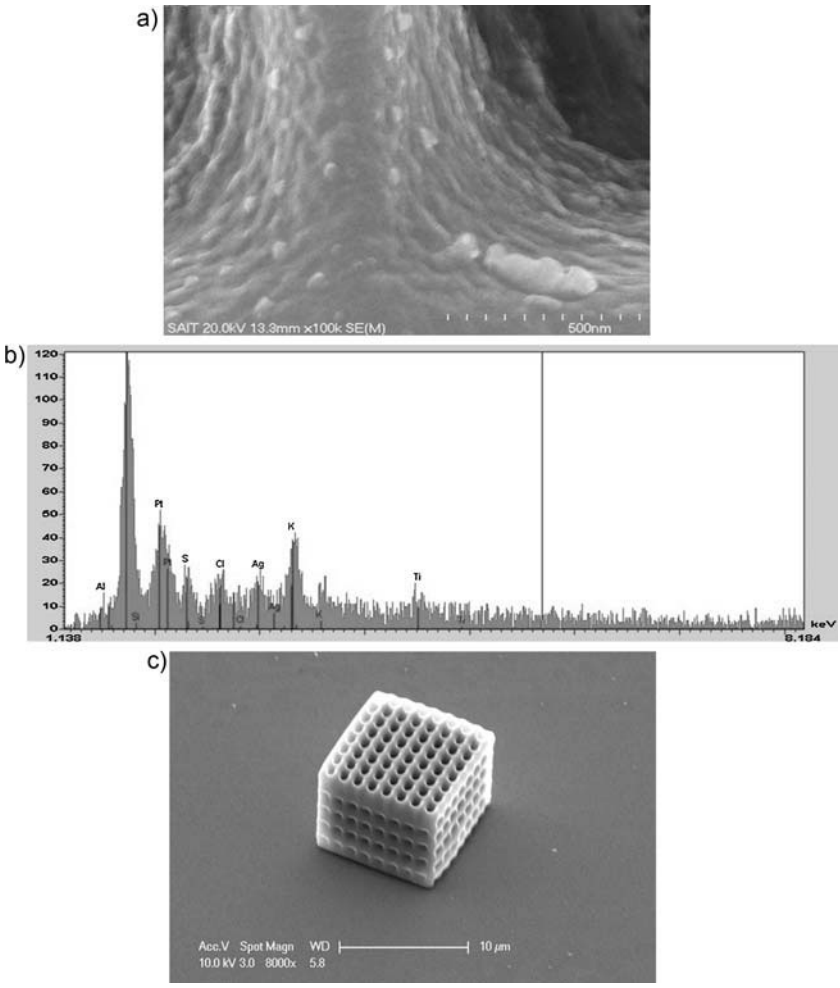

Figure 6. a) SEM image of the silver nanoparticles embedded on the 3D microfabricated surface (pattern composition of 0.2 wt% STA in SU-8) – silver particles on the pattern are uniformly distributed which prevents the collapse of 3D pattern, b) EDX spectrum of SEM image a – the existence of silver in the 3D pattern is confirmed by the EDX spectrum, and, c) SEM image of 3D microfabricated structure (0.2 wt% STA in SU-8 at 100 mW power).

inkjet heads[29] with heat dissipation in microchannels using the higher thermal conductivity of silver (430 W mK^{-1}). Further studies on the optimization of the concentration of nanoparticles generated are underway.

4. Experimental

Materials: Silver trifluoroacetate (STA), γ-butyrolactone (GBL) and the photoacid generator (triphenylsulfonium hexafluoro antimonate) used as cationic photoinitiator were purchased from Aldrich chemical company. The SU-8 (multifunctional epoxy resin) used in the microfabrications was procured from MCC and Hexion Specialty Co. All chemicals were used without further purification. A highly active spirofluorene-based two-photon absorption (TPA) dye [2′,7′-dibromo-3,6-bis(3,7-dimethyloctyloxy)-9,9′-spirobifluoren, 1 mg] was added to the well-mixed mixture to act as a two-photon photosensitizer (see the Supporting Information for details).

Preparation of 2D Microstructures: Commercial SU-8 epoxy resin, photoacid generator already mixed at ratios of 1–5 wt% and 2 wt% of STA were well mixed for 30 min. The mixture was then spin-coated at 2 000 rpm on a silicon wafer. The thin film was exposed to UV curing across a mask. UV curing was carried out at a rate of 13.6 mJ s^{-1} for 120 s (about 1 600 mJ cm^{-2}), or 240 s (about 3 200 mJ cm^{-2}). Post-exposure baking was carried out at 120 °C for 2 min and then the wafer was immersed in GBL for developing. 2D patterning was achieved with control of the developing time to optimize coating thickness and exposure time.

Preparation of 3D Microstructures: The 3D patterns were achieved through two-photon lithography, which involved an SU-8 resin containing photoacid generator dispersed with STA and sensitized with a highly efficient two-photon chromophore. For the two-photon lithography, a mode-locked titanium sapphire laser operating at 80 MHz with a central wavelength of 780 nm and pulse of duration less than 100 fs was utilized as the light source. A set of two Galvano mirrors was used to move the focused laser beam delicately in the horizontal plane, and a piezoelectric stage was used for the vertical alignment of the beam. The laser was closely focused into the volume of the resin placed on a thin glass plate using a high numerical aperture (1.4) objective lens (immersion oil used). A high magnification charge-coupled-device camera was used for the optical adjustment of the focused beam and monitoring the fabrication process.

Characterization: Microfabricated structures and some solutions were characterized by scanning electron microscopy (SEM, Hitachi, Ltd) to determine the dispersion and shape of silver nanoparticles within the SU-8 matrix. The surface morphologies of fabricated structures were observed by transmission electron microscope (TEM, Hitachi) at an accelerating voltage at 100 kV. UV-vis spectra (Varian 5000 UV-VIS-NIR spectrometer) were recorded by using a 1 cm quartz cell. FT-IR spectra(400–4 000 cm^{-1}) were recorded using a Perkin-Elmer FT-IR spectrophotometer with KBr windows. Thermal measurements were performed using a TA Instrument TGA 2050 and a TA Instrument DSC 2010. The total amount of residual metals in the samples was also estimated by TGA. UV was generated using a metal halide lamp (Ushio 250, Ushio Co.)

Acknowledgements

This work was supported by the Samsung Research Grant. K.-S. Lee acknowledges support from the National Research Foundation of Korea (NRF, Project No. 2010-0001696 & 2010-000499). D.-Y. Yang also thanks the Nano R&D Program through the NRF (M0300-21700) for financial support. T.-W. lee also acknowledges support of the Basic Research Program through the National Research Foundation of Korea (NRF) funded by the Ministry of Education, Science and Technology (No.2009-0075025). Supporting Information is available online from Wiley InterScience or from the author.

Received: January 11, 2010
Revised: March 4, 2010
Published online:

[1] T. Mitsui, Y. Wakayama, T. Onodera, Y. Takaya, H. Oikawa, *Nano Lett.* **2008**, *8*, 853.
[2] C.F., S. Murphy, I. Shvets, M. Porcu, H. W. Zandbergen, *Nano Lett.* **2008**, *8*, 3248.

[3] J. Huang, A. R. Tao, S. Connor, R. He, P. Yang, *Nano Lett.* **2006**, *6*, 524.
[4] M. P. Soriage, A. T. Hubbard, *J. Am. Chem. Soc.* **1982**, *104*, 3937.
[5] M. Brust, M. Walker, D. Bethell, D. J. Schiffrin, R. Whyman, *J. Chem. Soc. Chem. Commun.* **1994**, 801.
[6] J. H. Fendler, F. C. Meldrum, *Adv. Mater.* **1996**, *7*, 607.
[7] C. Chang, H. S. Fogler, *Langmuir* **1997**, *13*, 3295.
[8] A. Manna, B. D. Kulkarni, K. Babdyopadhay, K. Vijayamohanan, *Chem. Mater.* **1997**, *9*, 3032.
[9] Y. Xia, J. Tien, D. Qin, G. M. Whitesides, *Langmuir* **1996**, *12*, 4033.
[10] R. Maoz, S. R. Cohen, J. Sagiv, *Adv. Mater.* **1995**, *11*, 55.
[11] A. A. Avey, R. H. Hill, *J. Am. Chem. Soc.* **1996**, *118*, 237.
[12] S. Magdassi, A. Bassa, Y. Vinetsky, A. Kamyshny, *Chem. Mater.* **2003**, *15*, 2208.
[13] B. G. Ershov, E. Janata, A. Henglein, A. Fojtik, *J. Phys. Chem* **1993**, *97*, 4589.
[14] J. Pukies, W. Roebke, A. Henglein, G. B. Bunsen, *Phys. Chem.* **1968**, *72*, 842.
[15] T. R. Tausch, A. Henglein, J. Lillie, G. B. Bunsen, *Phys. Chem.* **1978**, *82*, 1335.
[16] B. K. Teo, K. Keating, Y. H. Kao, *J. Am. Chem. Soc.* **1987**, *109*, 3494.
[17] B. G. Ershov, N. L. Sukhov, D. I. Troiskii, *Radiat. Phys. Chem.* **1989**, *39*, 127.
[18] B. G. Ershov, E. Janata, A. Henglein, *J. Phy. Chem.* **1993**, *97*, 339.
[19] Y. F. Lu, M. Takai, S. Nagatomo, K. Kaito, S. Namba, *Appl. Phys. A: Mater. Sci. Process.* **1992**, *54*, 51.
[20] Y. F. Lu, M. Takai, T. Shiokawa, Y. Aoyagi, *J. Appl. Phys.* **1994**, *33*, 1313.
[21] E. P. Szlyk, P, A. Grodzicki, M. Chaberski, A. Golinski, J. Szatkowski, T. Blaszczyk, *Chem. Vap. Deposition* **2001**, *7*, 1.
[22] M. Quinten, *Appl. Phys. B: Lasers Opt.* **2001**, *73*, 317.
[23] N. Pradhan, N. R. Jana, K. Mallick, T. Pal, *J. Surf. Sci. Technol.* **2000**, *16*, 188.
[24] F. Stellacci, C. A. Bauer, T. Meyer-Friedrichsen, W. Wenseleers, V. Alain, S. M. Kuebler, J. K. S. Pond, Y. D. Chang, S. R. Marder, J. W. Perry, *Adv. Mater.* **1995**, *14*, 194.
[25] P. V. Kamat, M. Flumiani, G. V. Hartland, *J. Phys. Chem. B* **1998**, *102*, 3123.
[26] Y. Niidone, A. Hori, H. Takahashi, S. Yamada, *Stud. Surf. Sci. Catal.* **2001**, *132*, 359.
[27] K. Buscha, G. Freymann, S. Linden, S. F. Mingaleev, L. Tkeshelashvili, M. Wegener, *Phys. Rep.* **2007**, *444*, 101.
[28] M. S. Rill, C. Plet, M. Thiel, I. Staude, G. Freymann, S. Linden, M. Wegener, *Nat. Mater.* **2007**, *7*, 543.
[29] C. Linda, M. Marlene, *Mater. Res. Bull.* **2003**, *November*, 807.